MODELING OF NEAR-FIELD SCANING IN MATLAB

Roman Tkadlec

Department of Radio Electronics, Brno University of Technology

Abstract

This paper provides a theory of determination antenna far-field pattern from near-field measurements over a plane-rectangular surface. Implementation of this method to MATLAB has been solved and computed results were compared with theoretical values. A nine-dipole antenna has been chosen for the simulation.

Introduction

Near-field measurement is used for very large antennas for which the far-field distance becomes too large to fit within actual test range or an anechoic chamber. Near-field measurements provide a fast and accurate method of determining the antenna gain, pattern, polarization, beam pointing etc. The planar near-field technique is an effective method for measuring the performance of large antennas and other advanced low sidelobe antennas. The advantage of near-field measurements is a complete characterization of the antenna performance. In this paper is shown the whole process of near-field measurement for a nine-dipole antenna.

Near-field basics

We consider here an ordinary antenna radiating into free space (but not superdirective antenna). The space surrounding the antenna (Fig. 1) is conventionally divided into two main regions:

- In the far-filed region, which extends all the way to infinity, electric and magnetic fields decay at rate of $1/r$, where r is the distance from the antenna. The angular variation of the fields does not depend on this distance. The inner radius of the far field is approximately equal to the Fraunhofer distance $2D^2/\lambda$, where D is the main dimension of the antenna and λ is the wavelength in free space [4].

- The free-space region between the antenna and the far field is called near-field region. The radial and the angular dependence of the fields vary in a more complex fashion with distance within this region, so that mathematical transforms become necessary to determine the field at location when measurements been made elsewhere.

- The near-field region itself can be further subdivided into two another subregions (Fig. 1). To the reactive or evanescent near-field region, which start on the surface of the antenna and ends usually at a distance of one wavelength λ [4]. And to radiating near-field region which extends from the reactive region out to the far-field region. In this region we do the near-field measurements.
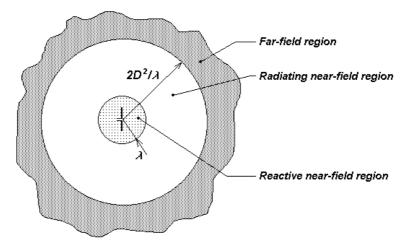
Fig. 1: Division of the space surrounding the antenna

Near-field scanning theory

All near-field measurement systems compute the various directions in which the electromagnetic energy is propagating. These directions of propagating are completely independent of distance to the antenna under test (AUT). The near-field measurement system operates by measuring the phase front of the AUT and then mathematically transforming the phase front into the equivalent far-field angular spectrum. For a planar near-field, the phase front and angular spectrum are related by a two-dimensional Fourier transform.

In our case we suggest an ideal scanning probe moving over a plane-rectangular surface (Fig. 2). That means we do not have to do any probe corrections.
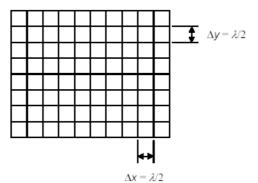

Fig. 2: Plane-rectangular scanning surface

The plane-rectangular scan area should accomplish the following:

- Must be large enough to accept all significant energy from the AUT. The correct scan dimensions can be determined by this expression

$$height(lenght) = D + 2 \cdot Z \tan \theta ,$$ (1)

where D is an antenna height (length), Z is an AUT – probe distance and the θ is a maximum processing angle from boresight [1].

- The discrete positions in which the probe will sample the near field must be exactly defined and satisfy the Nyquist sampling theorem.

- The sample points normally are arranged in a two dimensional grid (Fig. 2).

- The scan pattern should not be any denser than required by Nyquist criteria. This will minimize data acquisition time and storage requirements [1].

Far-field transformation algorithm for plane-rectangular scanning with an ideal probe

The transformation of phase front into an angular spectrum is often called a near-field to far-field transformation. Far-field can be evaluated by this expression (for ideal probe) [3]:

$$\mathbf{E}(x,y,z) = j\frac{e^{-jkr}}{r}k_z \cdot \mathbf{A}(k_x,k_y),$$ (2)

where r is a distance from scanning surface, $A(k_x,k_y)$ is called plane wave spectrum (PWS) and is given by

$$\mathbf{A}(k_x,k_y) = \int_{-\infty}^{\infty}\int_{-\infty}^{\infty}\mathbf{E}(x,y,0)e^{-jk_x x}e^{-jk_y y}\,dxdy\,,$$ (3)

where $E(x,y,0)$ is distribution of electric field over a scanning surface, k_x, k_y and k_z are a wavenumbers in x, y respective z direction and can be written as functions of angles θ and ϕ in spherical coordinate system.

$$k_x = k\sin\theta\cos\phi$$
$$k_y = k\sin\theta\sin\phi$$ (4)
$$k_z = k\cos\theta$$

Integrals in equation (2) can be replaced by sums for the set of n x m near-field samples measured on a plane-rectangular scan surface. Then we can write:

$$A(k_x,k_y) = \frac{1}{n}\sum_{i=1}^{n}\sum_{k=1}^{m}E_{i,k}(x,y,0)e^{-jk_x x_i}e^{-jk_y y_k}\,,$$ (5)

where $E_{i,k}(x,y,0)$ is complex sample of E on scan surface and x_i and y_k are probe positions for this sample. Finally the far-field in spherical coordinate system and for the discrete PWS is given by

$$E(\theta,\phi,z) = j\frac{e^{-jkr}}{r}k_z \cdot A(k_x,k_y),$$ (6)

Plane-rectangular near-field measurement simulation in Matlab

Firstly has been constructed a mathematical model of a nine-dipole antenna and then were computed samples of the electric field over a whole scanning surface. The set of samples represent a near-field measured with an ideal probe.

At the second the samples are transformed to the far-field and spatial frequency spectrum $A(k_x,k_y)$ is converted to an angular spectrum A of angles θ and ϕ.

At the last the angular spectrum $A(\theta,\phi)$ is multiplied by a wavenumber k_z and compared with theoretical results.

Nine-dipole antenna model

Antenna consists of nine dipoles and lye in *x-y* plane as is shown in Fig. 3. The dipoles have spacing $\lambda/2$ and each dipole is $\lambda/4$ long. All dipoles are feed with the current 1 A and phase shift between dipoles is 0°. Scanning surface with dimensions 20λ x 20λ lye at a distance $z_0 = 3\lambda$ from AUT and is coplanar with *x-y* plane (Fig. 3). The sampling points are spaced $\lambda/2$ apart and cover the whole scanning surface. Samples of the near-field have been evaluated according this expression:

$$E_{near} = 60 \cdot F_d(\theta,\phi) \sum_{i=1}^{N} I_i \frac{e^{-jkr_i}}{r_i} \tag{7}$$

where I_i is a current by *i*-th dipole and r_i is a distance from the *i*-th dipole to the actual sampling point, $F_d(\theta,\phi)$ is a radiation function for a symmetric dipole antenna and is given by [5]:

$$F_d(\theta,\phi) = \frac{\cos(kl\cos\phi) - \cos kl}{\sin\phi} \tag{8}$$

where *k* is a wavenumber, *l* is a length of the dipole and ϕ is an angle measured from the dipole axis.
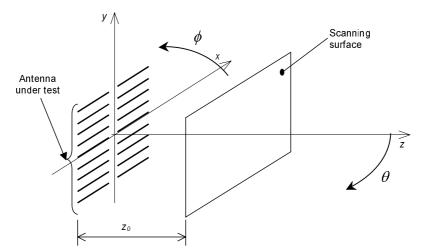

Fig. 3: Model of the nine-dipole antenna and its orientation in coordinate system

The source code of nine-dipole antenna is described below together with scanning area definition and with a kernel for near-field samples computation. Variables and constants definition is not listed.

```
%----------- scanning area definition -----------------------------------
velikostX = 20*lambda;        % size of the scanning area
velikostY = velikostX;
Nx = (velikostX/lambda)*2+3;  % samples at x axis
x = linspace(-(velikostX/2), (velikostX/2), Nx);
dx = abs(x(2)-x(1));
Ny = Nx;                      % samples at y axis
y = linspace(-(velikostY/2), (velikostY/2), Ny);
r0 = 2*lambda;                % distance of scanning surface from the AUT
```

```matlab
%------- testing antenna (AUT) definition (nine-dipole antenna) ----------
Nd = 9;                           % number of dipoles
dd = lambda/2;                    % dipole spacing
d = linspace((-(Nd-1)/2)*dd, ((Nd-1)/2)*dd, Nd);
I = ones(1,Nd);                   % currents for dipoles (1 A)
l = lambda/4;                     % dipole lenght
Fd = j*(cos(k*l)*cos(theta)-cos(k*l))/(sin(theta)); % radiation function of
                                                        symetric dipole

%----------- near-field samples computation ------------------------------
E = zeros(Nx,Ny);
Ehelp = zeros(1,Nd);      % help vector
for m=1:Ny
    for n=1:Nx
        for i=1:Nd
            E(n,m) = E(n,m) + 60*(cos(k*l*(x(n)/sqrt(r0^2+(y(m)-d(i))^2...
            +x(n)^2)))-cos(k*l))/(sqrt(r0^2+(y(m)-d(i))^2)/...
            sqrt(r0^2+(y(m)-d(i))^2+x(n)^2))*I(i)*(exp(-j*k*sqrt(r0^2...
            +(y(m)-d(i))^2+x(n)^2)/sqrt(r0^2+(y(m)-d(i))^2+x(n)^2));
        end
    end
end
Emax = max(E);
maxE = max(Emax);
Eneardb = 20*log(abs(E/maxE));

figure(1);                % 3D near-fiel distribution
surf(x/lambda,y/lambda,Eneardb);
title('Rozlozeni normovaneho modulu pole v blizke oblasti (z = 2*lambda)');
xlabel('y[lambda]');
ylabel('x[lambda]');
zlabel('abs(Enear)');

% depiction of E (module and phase) in the near-field for two orthogonal cuts

figure(2);
subplot(2,2,1);
plot(x/lambda,Eneardb(:,((Ny+1)/2)));
title('rez rovinou y = 0');
xlabel('x[lambda]');
ylabel('abs(Enear)');
subplot(2,2,2);
plot(y/lambda,Eneardb(((Nx+1)/2),:));
title('rez rovinou x = 0');
xlabel('y[lambda]');
ylabel('abs(Enear)');
subplot(2,2,3);
plot(x/lambda,angle(E(:,((Ny+1)/2)))/(2*pi)*360);
xlabel('x[lambda]');
ylabel('phase(Enear)');
subplot(2,2,4);
plot(y/lambda,angle(E(((Nx+1)/2),:))/(2*pi)*360);
xlabel('y[lambda]');
ylabel('phase(Enear)');
```

The corresponding x and y component of the amplitude and phase distribution over a scanning surface computed using expression (7) and source code above is shown in Fig. 4.
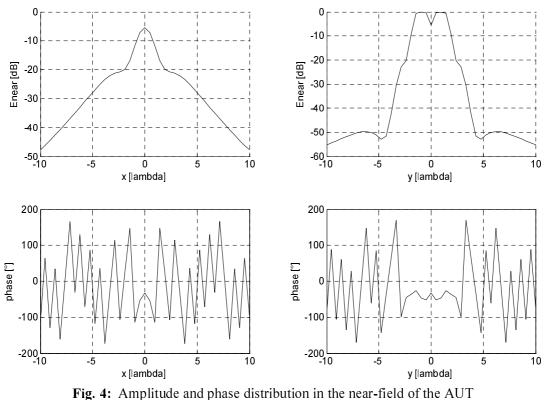
Fig. 4: Amplitude and phase distribution in the near-field of the AUT

Near-field to far-field transformation and conversion to an angular spectrum

Before that we do the transformation itself we must define angles where we like to compute the electric field E and fill it into equations (4). Now we can perform a 2-D Fourier transform for each combination of k_x and k_y. After transformation we simply convert the spatial frequency spectrum to the angular spectrum by using inverse equations to equations (4). Source code corresponding to this transformation is listed below.

```
----------- near-field to far-field transformation --------------------
A = zeros(t,t);          % spatial spectrum computation
for m=1:t
    for n=1:t
        for h=1:Ny
            for i=1:Nx
                A(n,m) = A(n,m) + E(i,h)*exp(j*k*(x(i)*kx(n,m)+y(h)*ky(n,m)));
            end
        end
    end
    t-m
end
A = A/(Nx*Ny);
```

Comparison of transformed near-field with theoretical results

The last step to reach the radiation pattern in the far-field from a set of near-field samples is multiplying the angular spectrum $A(\theta,\phi)$ by a wavenumber in z direction k_z. After this procedure we observe far-field pattern of the AUT (Fig.6 − solid line) for two orthogonal cuts ($\phi = 0°$ -
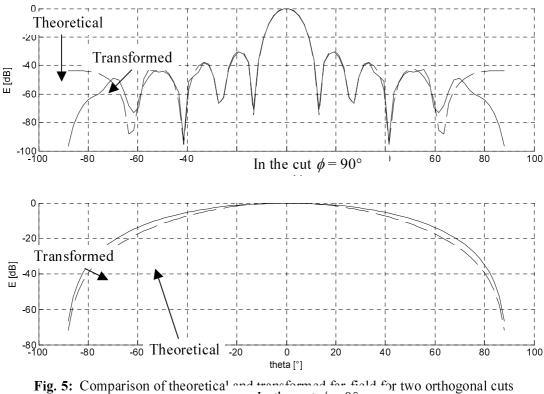
down and $\phi = 90°$ - up). Theoretical radiation pattern of the AUT consisting of nine dipoles (Fig. 4) is evaluated according expression [5]:

$$F(\theta,\phi) = \frac{\cos(kl\cos\phi) - \cos kl}{\sin\phi} \cdot \frac{\sin\left(\dfrac{N_d}{2}kd\cos\left(\theta + \dfrac{\pi}{2}\right)\right)}{\sin\left(\dfrac{1}{2}kd\cos\left(\theta + \dfrac{\pi}{2}\right)\right)} \tag{9}$$

where N_d is a number of dipoles and d is spacing between dipoles. Source code for theoretical radiation pattern is listed below.

```
% ------ far-field computation (theoretical values for comparison) -----------
Evzdal = zeros(t,t);
for m=1:t
    for n=2:(t-1)
        Evzdal(m,n) = ((cos(k*l*cos(phi(n)))-cos(k*l)) / sin(phi(n)))...
      *(sin(Nd/2*k*dd*cos(theta(m)+pi/2)))/(sin(1/2*k*dd*cos(theta(m)+pi/2)));
    end
end
Evzdalmax = max(Evzdal);
maxEvzdal = max(Evzdalmax);
Evzdal = abs(Evzdal/maxEvzdal);
Evzdaldb = 20*log(Evzdal);
figure(3);
surf(phi/(2*pi)*360,theta/(2*pi)*360,Evzdaldb);
title('Vyzarovaci diagram ziskany vypoctem');
xlabel('phi[°]');
ylabel('theta[°]');
zlabel('abs(Efar)');

% -------- multiplying the angular spectrum by a wavenumber ------------------
for i=1:t
    A(i,:) = kz.*A(i,:);
    A(:,i) = rot90(kz).*A(:,i);
end

Amax = max(A);
maxA = max(Amax);
A = A/maxA;
F = abs(A);
Fdb = 20*log(F);

figure(4);        % depiction of spatial spectrum for two orthogonal cuts
subplot(2,1,1);
stem(ky(:,45),abs(A(:,45)));
title('Rez prostorovym spektrem v rovine kx=0');
xlabel('ky');
ylabel('abs(A)');
subplot(2,1,2);
stem(kx(45,:),abs(A(45,:)));
title('Rez prostorovym spektrem v rovine ky=0');
xlabel('kx');
ylabel('abs(A)');

figure(6);          % theoretical and transformed values comparison
subplot(2,1,1);
```

```
plot(theta(2:(t-1))/(2*pi)*360,Evzdaldb(2:(t-1),45),'b',theta(2:(t-
1))/(2*pi)*360,Fdb(2:(t-1),45),'r');
xlabel('theta[°]');
ylabel('abs(Evzdal/Emax)');
subplot(2,1,2);
plot(theta(2:(t-1))/(2*pi)*360,Evzdaldb(45,2:(t-1)),'b',theta(2:(t-
1))/(2*pi)*360,Fdb(45,2:(t-1)),'r');
xlabel('phi[°]');
ylabel('abs(Evzdal/Emax)');
```


In the cut $\phi = 90°$

In the cut $\phi = 0°$

Fig. 5: Comparison of theoretical and transformed far-field for two orthogonal cuts

As we can see on Fig. 5 very good agreement with theoretical pattern (dashed line) over main lobe and first two side lobes was reached. At a third side lobe is maximum error slightly greater than 3 dB. Here is good to say that the scanning area is about five times larger than a greatest dimension of the AUT that means on a frequency of 3 GHz we must use a scanning area with dimensions 2 m x 2 m for this AUT.

CONCLUSION

Near-field measurements provide fast and accurate method for the measurements of the large antennas that cannot be fit to an anechoic chamber or antennas, which have the far-field region to far. Plane-rectangular scanning is more frequently used in near-field measurements than cylindrical and spherical scanning because most directive antennas have in near-field aperture distribution slightly larger than the projected area of the antenna and of course the setup of planar scanning is very simple and transformation near-field to far-field is relatively easy. This method provide very accurate results for antennas which has most of the electromagnetic energy concentrated in a spatial angle of c. 120° (Fig. 5). For less directive antenna is better use

cylindrical or spherical scanning.

Theory of plane-rectangular scanning and the process of evaluation radiation pattern from a set of near-field samples have been described. The transformation of the near-field to far field has been shown on the example of nine-dipole antenna and whole configuration has been implemented to MATLAB, results have been compared with theoretical values as well.

ACKNOWLEDGEMENT

REFERENCES

[1] SLATER, D.: *Near-Field Antenna Measurements*, Boston, Artech House 1991, ISBN 0-89006-361-3

[2] YAGHJIAN, A.D.: An Overview of Near-Field Antenna Measurements, *IEEE Transactions on Antennas and Propagation*, Jan. 1986, vol. 34, No.1, pp. 30 − 45

[3] WANG, J.J.H.: An Examination of the Theory and Practices of Planar Near-Field Measurement, *IEEE Transactions on Antennas and Propagation*, June 1988, vol. 36, No.6, pp. 746 − 753

[4] BOLOMERY, J.C. − GARDIOL, F.E.: *Engineering applications of the modulated scatterer technique*, London, Artech House 2001, ISBN 1-58053-147-4

[5] CERNOHORSKY, D. − NOVACEK, Z.: *Navrhovani radiovych spoju*, Brno, VUT 1992, ISBN 80-214-0382-9

Contact

tkadlec@tut.fi
Department of Radio Electronics
Brno University of Technology
Purkynova 118
612 00 Brno